Environ Earth Sci (2015) 74:1303–1318
DOI 10.1007/s12665-015-4120-5

ORIGINAL ARTICLE

Hydrogeological vulnerability and pollution risk mapping of the Saq and overlying aquifers using the DRASTIC model and GIS techniques, NW Saudi Arabia

Izrar Ahmed · Yousef Nazzal · Faisal K. Zaidi · Nassir S. N. Al-Arifi · Habes Ghrefat · Muhammad Naeem

Received: 2 June 2014 / Accepted: 26 January 2015 / Published online: 14 February 2015

Abstract Saq and overlying aquifers serve as important sources of water supply for agricultural and domestic usage in Saudi Arabia. Due to urbanization and growth in the agricultural sector, groundwater resources are over-exploited and are prone to quality deterioration. The aquifer vulnerability technique helps delineate areas according to the susceptibility to groundwater contamination. Various parameters pertaining to the surface and subsurface environment were synthesized to represent the data variation in the 3D horizon. Estimates of the parameters, such as recharge, soil media, and vadose zone, were obtained based on modified criteria to account for data variability. Statistical analysis indicates that the input parameters are independent and contribute individually to the vulnerability index. For vulnerability assessment, the DRASTIC model was considered due to the large number of data input parameters. Based on the vulnerability index, the study area is classified into low to very high vulnerability classes. To assess the human interaction on the groundwater environment, the land-use pattern was included as an additional input layer. Sensitivity analyses helped to compute the influence of the input layers on the vulnerability index and the model calibration through revised weights. The model validity tests were performed by comparing the NO_3, SO_4 and Cl concentration with the different vulnerability zones. The aquifer vulnerability maps developed in the present study may serve as an important tool for effective groundwater resource management.

Keywords Recharge potential · Arid region · Groundwater pollution · Aquifer vulnerability · Saudi Arabia

I. Ahmed (✉)
Water Resources, Civil Engineering Department, College of Engineering, King Saud University, Riyadh 11451, Saudi Arabia
e-mail: izrarahmed@yahoo.co.in; izrarahmed@gmail.com

Present Address:
I. Ahmed
ArRiyadh Development Authority, Riyadh, Saudi Arabia

Y. Nazzal · F. K. Zaidi · N. S. N. Al-Arifi · H. Ghrefat · M. Naeem
Department of Geology and Geophysics, College of Science, King Saud University, Riyadh 11451, Saudi Arabia

Y. Nazzal
Department of Applied Mathematics and Sciences, College of Arts & Sciences, Abu Dhabi University, 59911 Abu Dhabi, UAE

Introduction

Due to the limited groundwater resources, scarce rainfall, and very high mean evaporation, Saudi Arabia is considered to be one of the driest countries in the world. Rapid industrialization and agricultural advancements have led to unsustainable groundwater abstraction and water quality deterioration. In the past few decades, groundwater contamination has emerged as a serious environmental problem. Although, to some extent, the physical environment provides protection to the groundwater (Vrba and Zaporotec 1994), the extent of the protection could be variably uncertain. Regardless, protection of groundwater resources from contamination requires a thorough understanding of the groundwater environment.

The Saq and overlying aquifers, located in the northwest part of Saudi Arabia serve as important sources of water supply, primarily for agriculture and domestic use. Groundwater trapped mostly in Paleozoic and Mesozoic sedimentary formations exhibits high salinity acquired through rock–water interaction during the long resident

time period. The high concentration of NO_3 in the groundwater indicates recent contamination from surface activities, primarily agriculture and city sewages (Nazzal et al. 2014a, b). In addition, in the last two to three decades, the study area has witnessed high human and infrastructural developments, which have resulted in the excessive abstraction of Saq and the overlying aquifers (MoWE 2008; Al-Salamah et al. 2011). Studies have documented groundwater quality deterioration primarily due to prolonged rock–water interaction and anthropogenic influences, including increased usage of chemical fertilizers (Sawayan and Allayla 1989; Al Bassam 2006; MoWE 2008; El Maghraby et al. 2013; Nazzal et al. 2014a). Considering these factors, it became necessary to perform a pollution assessment study of the underlying aquifers to determine its vulnerability to contamination. The results of the study will assist the policy makers in the proper management of the available groundwater resources by restricting the activities contributing to groundwater pollution in the highly vulnerable zones.

Groundwater resources are often studied to address qualitative and quantitative issues. Groundwater pollution has become a serious environmental problem, primarily due to increased human interaction with the groundwater environment (Mendizabal and Stuyfzand 2011; Güler et al. 2012). The best preventive measures require delineation of the area on the basis of susceptibility to contamination. Vulnerability assessment, basically a subjective concept, is based on the fact that some land areas are more vulnerable to groundwater contamination than others (Vrba and Zaporotec 1994), depending upon their hydrogeologic nature. The vulnerability assessment does not account for the characteristics of the pollutants. In recent years, groundwater vulnerability assessment has become a very useful tool for the planning and decision-making involving groundwater protection (Gogu and Dassargues 2000; Vias et al. 2006; Huan et al. 2012). The vulnerability assessment technique includes the overlay-index method (Neshat et al. 2014), the statistical method (Sorichetta et al. 2011 and the process-based method (Milnes 2011). Numerous studies have been performed to systematically evaluate the potential of a hydrogeological environment to pollution contamination. Some of these methods include DRASTIC (Aller et al. 1987), GOD (Foster 1987), AVI (Van Stempvoort et al. 1993), SINTACS (Civita 1994), SEEPAGE, EPIK (Doerfliger and Zwahlen 1997) and ISIS (Navlur and Engel 1997). These methods integrate various hydrological and hydrogeological parameters in different combinations set by ratings and weights. Nevertheless, all of the methods were mainly used to assess groundwater vulnerability to contamination.

The DRASTIC method, which is an overlay-index method, is a widely used technique for vulnerability assessment (Aller et al. 1987; Evans and Myers 1990; Rosen 1994; Babiker et al. 2005; Rahman 2008) that integrates seven physical and hydrodynamic parameters. Some researchers modified DRASTIC by adding parameters such as land-use pattern (Al Hanbali and Kondoh 2008; Umar et al. 2009; Alam et al. 2012) and the contaminant adsorption coefficient of sediment in the vadose zone (Qinghai et al. 2007). The accuracy of the DRASTIC parameters is the key to a successful model. Therefore, new estimation approaches are often used that can account for existing data variability within one parameter, differentiating between the nearly identical data types with only slightly differing characteristics.

The present study aims at the detailed assessment of the aquifer vulnerability to contamination. The integrated use of GIS techniques and the hydrodynamic behavior of the study area have produced first-hand information on aquifer vulnerability, which policy makers can use for implementing policies for effective and sustainable groundwater usage.

Study area

The study area falls between 24° 09′N and 32° 00′N and 35° 35′E and 44° 30′E, forming the NW part of Saudi Arabia and covering an area of approximately 0.18 million km^2. Al Jawf, Al-Qassim and Tabuk are the main urban centers within the study area. The climate in northwestern Saudi Arabia is arid, with low annual rainfall and high evaporation. Nevertheless, some regional differences exist, with the lowest mean annual rainfall (<30 mm/year) in the western part of the area and the highest rainfall in the southeastern part (170 mm/year). With such a low average rainfall and a high potential evaporation of nearly 2,400 mm/year, the groundwater recharge can only occur at favorable sites. The temperature ranges from 43 to 48 °C during daytime and 32 to 36 °C during nighttime in summer.

The study area hosts significant agricultural tracts unevenly distributed as clusters at places for specific reasons, such as alluvial Wadis track and groundwater availability. During the past three decades, tremendous growth in agricultural activities has triggered groundwater abstraction. The total volume of groundwater abstracted in the Saq area in 2005 (8,727 Mm^3/year) equals a water column of 24 mm covering the entire Saq area. Such a volume is five to ten times higher than the recharge occurring during the same period and is therefore not sustainable (MoWE 2008).

Geology and hydrogeological framework

The Arabian Peninsula can be divided into two main geological units: the Precambrian shield in the western part and the Arabian Shelf in the eastern and central part. The Arabian shield is composed of Proterozoic basement rocks.

The Arabian shield consists of igneous, metamorphic, metavolcanics, metasedimentary, and other varieties of basement complex rocks. The youngest basement complex rocks, which precede the Paleozoic, have been assigned the age of less than 600 Ma before present (Brown et al. 1989). The sedimentary platform consists of Phanerozoic rocks that extend hundreds of kilometers eastward of the Arabian shield until they reach the Arabian Gulf.

During the Paleozoic era, the most extensive transgression activities took place during the early Ordovician (Upper Saq sandstone Formation) that covered the northwestern and eastern edge of the Arabian Shield. The southern edge of the Hanader shale transgression lies in the Tabuk and Ha'il regions, while the Devonian one (Al Jawf formation) was more limited to the Al Jawf region (Al Huj group, Tawil, Al Jawf and Al Jubah formations) (Fig. 1b). Paleozoic rocks were deposited as fluviatile braided river environment (Al-Dabbagh and Rogers 1983) in three main zones. These three zones are located in the Northwest Saudi Arabia (Tabuk region), Central Saudi Arabia (Qassim region), and Southwest Saudi Arabia. Paleozoic formations are important in Saudi Arabia because they form important water aquifers and are located in three zones of outcrops deposited in an arch surrounding the pre-Cambrian Arabian shield between Jordan in the northwest and Yemen in the south. These three zones are located in Northwestern Saudi Arabia (Tabuk region), Central Saudi Arabia (Qasim region), and Southwestern Saudi Arabia.

Hydrogeologically, there are seven aquifers or aquifer groups moving away from the contact with the basement toward the east, and the overlying formations appear one after the other in chronological order (MoWE 2008). The last two layers act regionally as aquitards, but contain units that are locally exploited as aquifer (Table 1):

Methodology

The DRASTIC method is based on weights and ratings associated with seven hydrogeological parameters. These parameters are depth to groundwater table (D), net recharge (R), aquifer media (A), soil media (S), topography (T), impact of vadose zone (I), and hydraulic conductivity (C). Each parameter is assigned a unique weight (w_i) and rating (r_i). The weight factor ranges from 1 to 5, corresponding to a significance scale from the lowest to the highest. The ratings of the data may vary depending on the type, frequency, and range, thus making the model function in a site-specific manner. The linear additive combination of the above parameters with weights and ratings was used to calculate the DRASTIC vulnerability index (DVI), as given below (Aller et al. 1987):

$$\mathrm{DVI} = D_r D_w + R_r R_w + A_r A_w + S_r S_w + T_r T_w + I_r I_w + C_r C_w, \quad (1)$$

where the suffixes r and w represent the rating and the weight assigned to each parameter. In the present study, the

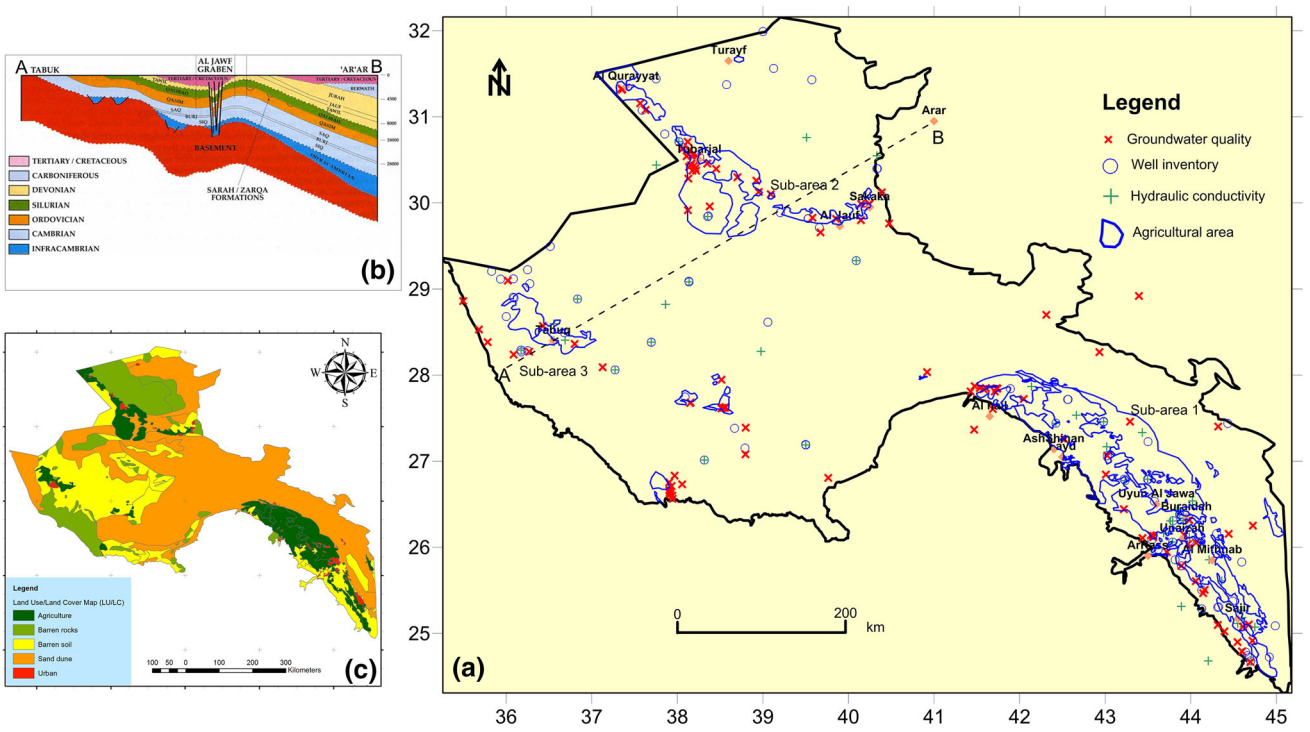

Fig. 1 Base map of the study area showing **a** various locations, **b** inset geological cross section, and **c** land-use categories of the study area

DRASTIC model (Aller et al. 1987) was further modified by the unique rating classes of each parameter relevant to the study area. The land-use map with five classes was selected to account for their role in the groundwater contamination. For the land-use classes, a satellite image (MOD09A1 data) was acquired on January 2014. The Moderate Resolution Imaging Spectroradiometer (MODIS) Surface MOD09A1 provides Bands 1–7 at 500-m resolution in an 8-day gridded level-3 product in the Sinusoidal projection. Various maps, including the land-use map, were prepared using Arc GIS 10 with an average grid size of 1 km. ArcGIS 10 helps in data extraction, rasterization, kriging and contouring, math, and combining various layers.

The map removal sensitivity analysis (Lodwick et al. 1990) is computed as a variation index (%):

$$S = \left| \frac{V_{\mathrm{i}}}{N} - \frac{V_{\mathrm{xi}}}{n} \right| \times 100/V_i, \quad (2)$$

where S is the sensitivity index, V_{i} is the vulnerability index, N the number of map layers used for computing V_{i}, V_{xi} the vulnerability index excluding one map layer, and n the number of maps used for calculating V_{xi}.

The variation index, which refers to the variation in the magnitude produced by removing one map layer (corresponding to one parameter), is computed as

$$V = \left[\frac{V_{\mathrm{i}} - V_{\mathrm{xi}}}{V_{\mathrm{i}}} \right] \times 100, \quad (3)$$

where V is the variation index of the removed parameter, V_{i} the vulnerability index computed using Eq. 1, and V_{xi} the vulnerability index calculated excluding one map layer.

The single parameter sensitivity analysis introduced by Napolitano and Fabbri (1996) is computed as

$$W = \left(\frac{P_{\mathrm{r}} P_{\mathrm{w}}}{V} \right) \times 100, \quad (4)$$

where W is the effective weight of the parameter P, P_{r} the rating, P_{w} the weight, and V the vulnerability index.

Conceptualization of the DRASTIC model

The data acquisition step is crucial, as a limited data type could lead to inaccurate results. The data used for various input parameters were procured from different techniques and sources (Table 2). The geographic extents of the study area were set, and the data acquisition for each parameter was later transformed to construct a 1-km^2 grid size (total of 21,086 grids). The distributed data contours are transformed into ranges corresponding to which ratings are assigned on the basis of the relative likelihood to contamination. Because the data range depends on the local geology and hydrogeology, the rating can differ from one study area to another.

Depth to the water level

The depth to the water level determines the migration distance that a contaminant will travel before reaching the aquifer. Therefore, the contaminant will take a relatively longer time to reach a deep water level compared to a shallow water level. In addition, the deeper the water level, the higher is the attenuation capacity of the geologic material (Aller et al. 1987; Civita 1994). In this study, the depth to the water level was measured at approximately 200 piezometers. The depth of the first occurrence of the water level was taken as the water level that was utilized to generate the depth to the water level map. The depth water level contour map and its index map are shown in Fig. 2.

Potential groundwater recharge

The groundwater recharge estimates using various techniques, including Darcy's law, chloride mass balance, and ^{14}C-isotopes, exhibit an average value of 4.2 mm/year. At the scale of the entire Saq area, the groundwater recharge is variable and does not exceed 5 mm/year (MoWE 2008b). Assuming a uniform recharge to the entire study area could

Table 1 Depth to water range and average conductivity of the hydrogeological formation

Hydrogeological formation	Depth to water level (m)	K (m/d)
Saq sandstone	65–297	4.36
Kahfah sandstone	30–250	9.5
Quwarah–Sarah sandstones	85–240	0.864
Sharawra sandstones	120	21.64
Jubah sandstone	120–150	0.56
Khuff limestone	192–250	4.36
STQ sandstone and limestone	15–290	17.49
Jauf limestone and sandstone	130–250	0.86
Unayzah and Berwath sandstones		

Table 2 DRASTIC parameters

DRASTIC parameters	Modification (if any)	Range	Ratings	Weight	Data source
Depth to water		0–25	10	5	Field measurements, MoWE (2008)
		25–50	9		
		50–100	7		
		100–150	5		
		150–200	3		
		200–250	2		
		>250	1		
Recharge (potential)	Integration of four data layers (geology/drainage/slope/ rainfall)		1–10	4	Geological map of NW Saudi Arabia SRTM (90 m) slope and drainage Rainfall data (MoWR)
Aquifer media		Shale	3	3	Geological map and hydrogeological formation map (BRGM 2005; MoWR)
		Wadi beds, mixed lithology	5		
		Mixed sandstone/limestone	6		
		Dolomite/sandstone/ evaporite/clastics	7		
		Sandstone	8		
		Coarse sandstone	8		
		Sanddunes, alluviums	10		
Soil media	Integration of 5 soil parameters (thickness/type/use/water retention, conductivity)	Loamy	1	2	Water atlas
		Loamy-sand	3		
		Loamy-rocky	5		
		Sandy clay	7		
		Sandy	10		
Topography		<1 (degree)	10	1	SRTM (90 m)
		1–2	9		
		2–4	8		
		4–6	7		
		6–12	5		
		12–18	3		
		>18	1		
Impact of vadose zone	Harmonic mean of successive layers	Loam	1	5	Lithologs from MoWE (2008) and other Literature
		Siltstone	2		
		Chert/shale/clay	3		
		Sandstone/limestone	6		
		Dolomite	8		
		Sand	9		
Conductivity	Average conductivity of each formation	0–3 (m/day)	1	3	Old literature, BRGM 2005, MoWE 2008, personal communications with senior professionals, KACST
		3–6	3		
		6–9	5		
		9–12	7		
		>12	10		

be potentially erroneous. Therefore, attempts have been made to estimate the groundwater recharge potential rather than the actual recharge. The recharge potential estimation includes detailed geology, drainage pattern, topographic slope, and rainfall amount. The geology of an area acts to control the migration of contaminants into the aquifer through filtration, sorption, cation exchange, and other processes (Soller and Berg 1992). Because the geology controls the movement and quality of the groundwater, the nature of the overall formation is taken into account by a comparative rating among the different hydrogeological formations presented in the study area (Fig. 3a). A high

Table 3 Rating class criteria to different index parameter used to estimate groundwater recharge potential

Geology index		Drainage index		Slope index		Rainfall index	
Type	Rating	Type	Rating	Range	Rating	Range	Rating
Aquifer	10	Large	10	<1	10	150–170	10
Aquiclude	5	Medium	5	1–2	9	130–150	9
Aquitard	1	Small	2	2–4	8	110–130	8
Sabkha	1	No	1	4–6	7	90–110	7
				6–12	5	70–90	5
				12–18	3	50–70	3
				>18	1	0–50	1

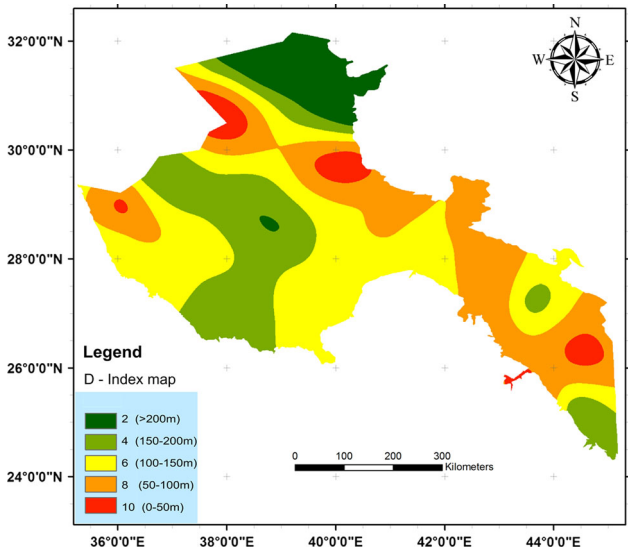

Fig. 2 Contour map showing depth to water level index map

rating assigned to a formation implies that it can behave as an aquifer, while a low rating indicates an aquiclude and aquifuge (Table 3).

Geomorphological features often help in identifying a suitable site for groundwater recharge (Chenini and Mammou 2010; Al Saud 2010). The drainage density is considered to be an important factor related to groundwater recharge. The high index value is assigned to areas exhibiting high drainage density, such as the northwestern and southeastern parts, while the middle part is dominated by sand dunes and the western part exhibits a low drainage density (Fig. 2b). Topography refers to the slope variability of land and often governs the general gradient and the direction of the flow of groundwater (Todd 1980; Aller et al. 1987). The slope may affect both the surface water and groundwater environment. The higher the topographic slope, the lower is the rate of infiltration; hence, a higher slope decreases the migration of contaminants. However, in the groundwater environment, the steeper slope signifies a high groundwater velocity, which in turn can increase the migration of contaminants. The slope map was derived from a digital elevation model (DEM) of 90-m resolution, obtained from the Shuttle Radar Topographic Mission (SRTM) and further classified into different rating classes (Fig. 3c).

Climatologically, the study area is characterized by a typical arid environment with low rainfall ranging from 50 mm/year in the west to 170 mm/year in the eastern part. The isohyets were assigned a unique class (Fig. 3d). The low-intensity rainfall restricts the groundwater recharge to selective sites where the concentration of runoff coincides with favorable sites, preferably wadi channels, alluviums, karst openings, etc. Selected studies from Saudi Arabia indicated a high rainfall recharge at small catchments (Memon et al. 1986; Subyani 2004) and favorable sites (Hoetzl 1995).

For the computation of the potential recharge, each of the parameters was converted to an index map by assigning a unique rating, depending upon its expected role in groundwater recharge (Table 3). The groundwater recharge potential (GW_R) can be represented as:

$$GW_R = (\text{Geology index} + \text{Drainage index} + \text{slope index} + \text{rainfall index})/4. \quad (5)$$

The recharge potential data layer was obtained after all of the four data layers were sum averaged in the GIS environment using Eq. (5), and then the average was scaled to uniform ratings from 1 to 10 (Fig. 3e).

Aquifer media and soil media

Aquifer media reflects the attenuation characteristics of the aquifer material, taking into account the mobility of the contaminant through the aquifer material. The lithologs are characterized to address vertical and horizontal lithological variability, and the interpolation of the point data performed to generate surfaces of particular hydrogeological formation. The ratings are based on a comparative assessment regarding how well a given formation would behave as an aquifer unit (Table 4; Fig. 4a). Soil media refers to the uppermost portion of the vadose zone, which is characterized by significant biological activity. The soil has

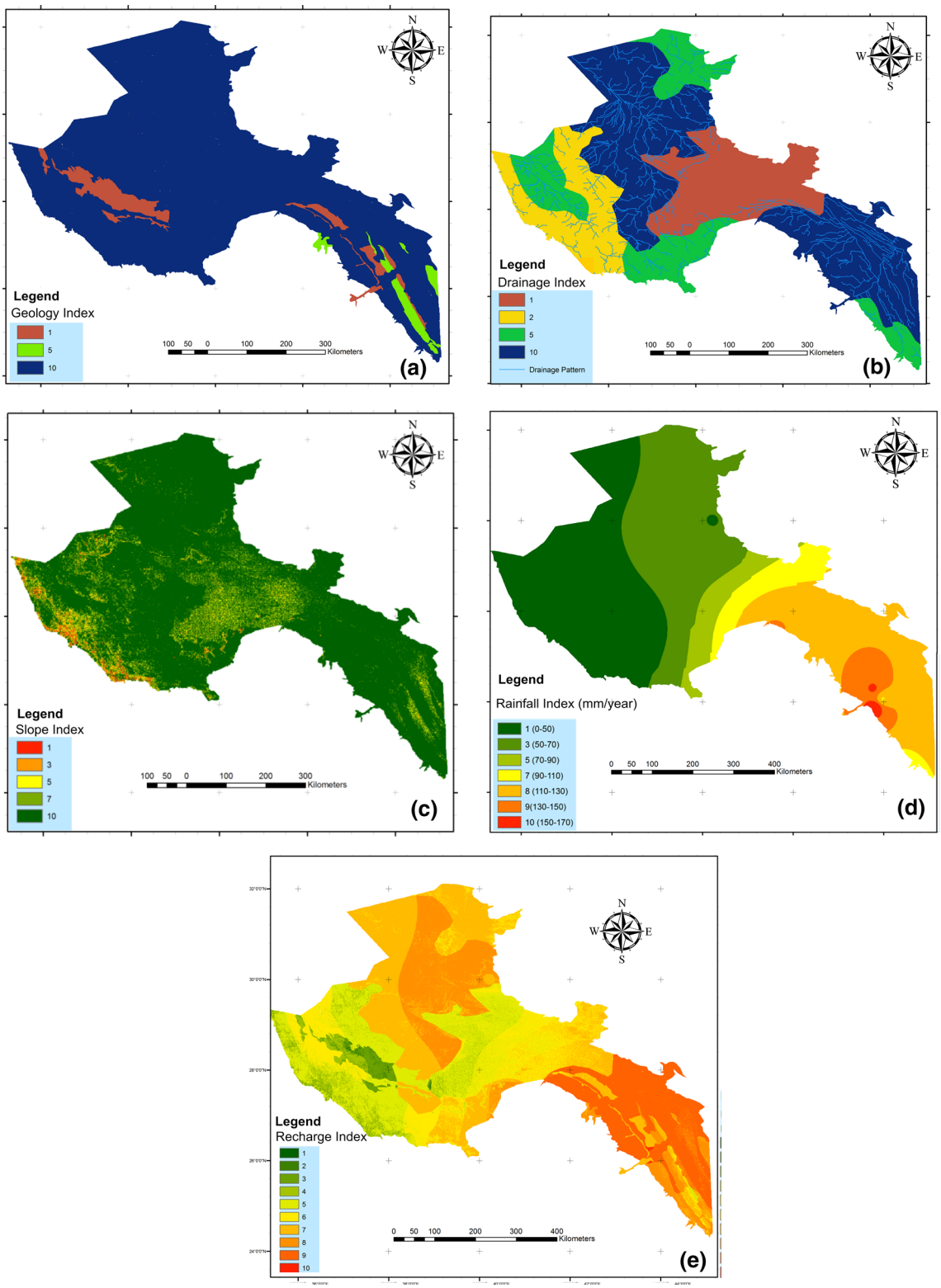

Fig. 3 Map showing integration of **a** geology index, **b** drainage index, **c** slope index, and **d** rainfall index to generate, **e** recharge potential map

a significant impact on the amount of recharge and on the ability of contaminants to move vertically into the vadose zone (Aller et al. 1987). Predominant soil types in the study area are Calciorthids-rock outcrops, Torriorthents and Torripsamments rock outcrops or sand dunes type. The former is basically loamy, arable soil found at gently

Table 4 Aquifer media rating class to various hydrogeological formations

Geological formations	Lithology	Rating
Qusaiba, Sudair, Qasim fm, Sabkha	Shale, evaporite	3
Jalamid, Mira, Sirhan, Qasim, Dhurma	Gradational sandstone/chert limestone	5
Sharawa, Jauf, Wasia, Jubailah, Hanifa, Marrat	Variable limestone/sandstone	6
Harrat, Jilh, Khuff, Zarqa	Basaltic flows/variable sandstone	7
Siq, Tawil, Qasim, Quweira, Jubah, Minjur, Biyadh, Qasim (Quwarah)	Sandstone	8
Alluviums, Saq fm	Alluv./sandstone	9
Sand dunes, sand–gravel deposits	Sand/gravel	10

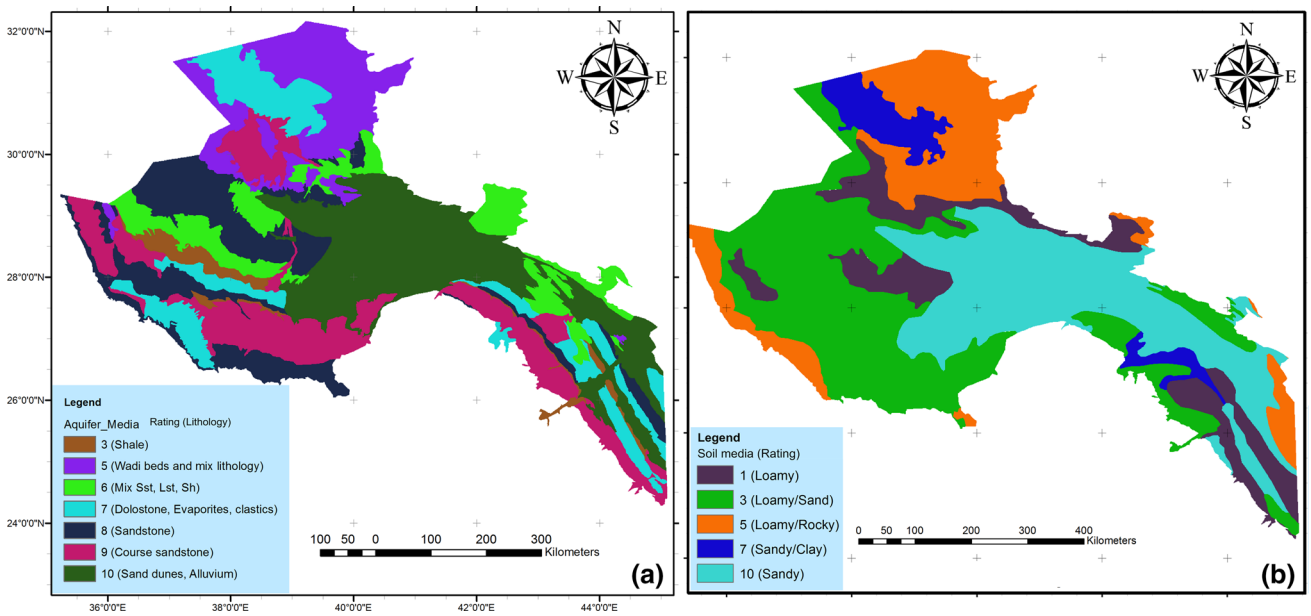

Fig. 4 Map showing the spatial distribution and rating criteria of **a** aquifer media and **b** soil media

sloping alluvial plains, fan piedmonts, and interfluve area. However, the latter is typically represented by sand dunes, i.e., it is a mix of sand, rock outcrop, and non-arable type (world Atlas 1984). To assign a suitable rating to each soil type, various soil parameters, such as thickness, use, water retention, and conductivity, were taken into account (Table 5). The spatial extents and distribution of the various soil types are shown in Fig. 4b.

Impact of the vadose zone and hydraulic conductivity

The vadose zone is an unsaturated zone above the water table. In the case of a confined aquifer, the impact of the vadose zone is expanded to include both the vadose zone and the overlying saturated layer. The vadose zone was evaluated using more than 100 lithologs. Various lithological units encountered in the lithologs are presented with their respective ratings. The material present in the vadose zone may vary significantly due to its hydraulic characteristics. To account for the variation in different materials in a litholog, the harmonic mean of the vadose zone was taken. This lithological log of more than 100 wells was divided into the above-mentioned classes, and the individual thicknesses of these layers were calculated. The rating of each lithology was assigned as mentioned above. The impact of the vadose zone (I_r) was calculated by the following formula:

$$I_r = \frac{T}{\sum_{i=1}^{n} T_i / I_{ri}}, \tag{6}$$

where I_r is the weighted harmonic mean of the vadose zone; T the total thickness of the vadose zone; T_i the thickness of the layer i; and I_{ri} the rating of layer i. The hydraulic conductivity controls the rate of groundwater movement into the saturated zone, thereby controlling the degree and fate of the contaminants. In the present study,

Table 5 Soil rating acquired through using 5 soil parameters

Nomenclature	Thickness	Type	Use	Avail. water cap.	Conductivity	Combined rating
Calciorthids–Cambriorthids	Deep	Loamy	Arable	mod./mod	Mod./mod	6.5
Calciorthids–Torripsamments	Deep	Loamy/sandy	Arable	mod./low	Mod./mod.	6.75
Gypsiorthids–Calciorthids–Torripsamments	Deep/low	Sandy/clay	Non-arable/arable	mod./low	Mod/mod/rap	7.25
Torripsamments	Low	Sandy	Non-arable	low	Rapid	8
Rock out crops–Calciorthids–Torriorthents	Mod.	Loamy/rocky	Non-arable	mod	Rapid	7

the hydraulic conductivity values obtained through the pump test results (MoWE 2008) were averaged and assigned to each formation.

Results and discussion

Vulnerability map

The correlations between the input data layers and the DVI indicate that parameters such as depth to water, recharge, aquifer media, and soil media are significantly correlated with DVI. Other parameters such as the impact of the vadose zone and the conductivity are moderately correlated with DVI. However, the topographic slope is poorly correlated with DVI. The readily used approach for vulnerability classification is based on the index range (Hussain et al. 2006; Jamrah et al. 2008; Umar et al. 2009; Edet 2014) rather than through the unique national color coding of the vulnerability maps (Aller et al. 1987). The DVI was computed after integrating seven data layers using GIS environment according to Eq. (1). The DVI scores classify the study area into four different classes of vulnerability potential (Fig. 5). The DVI scores are relative, area specific, and unitless in magnitude, where a higher DRASTIC index necessarily infers greater groundwater pollution (Umar et al. 2009; Edet 2014) and vice versa. These vulnerability zones, namely 70–100, 100–130, 130–160, and >160, correspond to low, medium, high, and very high vulnerability zones, respectively. The middle, south-east, and some areas in the NW part of the study area exhibit very high vulnerability zones, which constitute approximately 33 % of the total area. The vulnerability map reveals that the aquifer beneath the agricultural tracks of the SE part is in the category of high to very high vulnerability to pollution. The high scores of the parameters in this area, in particular the high scores of the recharge potential and the aquifer media, are responsible for the high vulnerability zone in this part. However, the NW part exhibits medium to high vulnerability. Generally, the DVI increases from the west to the eastern part of the study area.

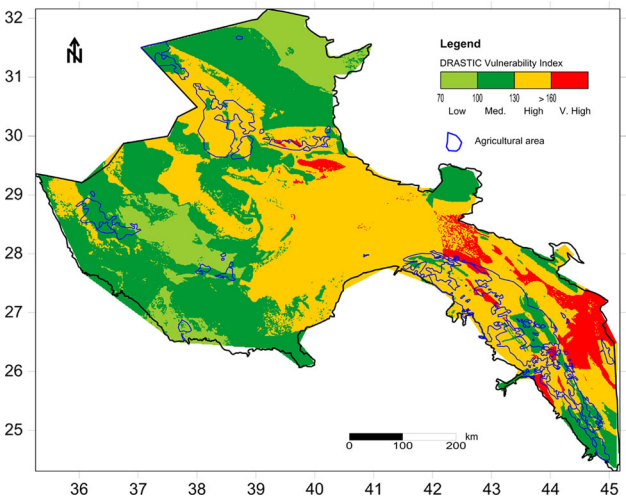

Fig. 5 DRASTIC vulnerability index (DVI) map

Table 6 A statistical summaries of the DRASTIC parameters

	Mean	Min	Max	SD	CV
D	4.94	0.93	10.00	1.96	39.68
R	6.67	2.05	9.83	1.53	22.95
A	7.81	2.48	10.00	1.89	24.15
S	5.26	0.41	10.00	3.23	61.43
T	8.85	1.09	10.00	1.38	15.55
I	5.06	2.75	7.86	0.57	11.30
C	3.23	0.27	10.00	2.71	83.88

DRASTIC parameters

The statistical summary of the seven DRASTIC input data layers is presented in Table 6. The highest risk of groundwater contamination could be inferred from the high mean rating of the topographic slope parameter (mean rating of 8.9). The presence of the aquifer media, the recharge, and the soil media imply a moderate risk of groundwater contamination, while the depth to water, the impact of the vadose zone, and the conductivity imply a low risk of aquifer contamination. The conductivity data, with a high coefficient of variation (CV% = 84.15), are

highly variable within the study area. The topographic slope and the impact of the vadose zone exhibit the least variability (CV% = 15.52 and 10.84, respectively).

The higher variability of the parameters implies a greater contribution toward the variation of the DVI. Conversely, the low variability of the parameter indicates a smaller contribution to the variation of the DVI. The low variability of the DRASTIC parameter could be either due to the simple natural setting or erroneous conceptualization. Due to the lack of significant correlations, the DRASTIC parameters can be termed as independent. The parameters, such as the aquifer media, the depth to water, and the soil media, exhibit good correlation with the DVI. Note that all of these three parameter layers were constructed using different procedures, as evident in their correlations: depth to water and aquifer media ($r = 0.22$), depth to water and soil media ($r = 0.14$), and aquifer media and soil media ($r = 0.34$). The DVI is least correlated with the topographic slope ($r = 0.01$).

Model sensitivity

The major advantage of the DRASTIC model lies in the consideration of a large dataset (Evans and Myers 1990), which also limits the impacts of the errors to the final output that may arise due to the individual parameter (Rosen 1994). Arguably, models with fewer input parameters may yield better accuracy (Merchant 1994). Being subjective in nature, the selection of the ratings and the weights may introduce errors to the final output. To analyze the model sensitivity, two techniques, i.e., the map removal sensitivity (Lodwick et al. 1990) and the single parameter sensitivity analysis introduced by Napolitano and Fabbri (1996), are commonly used. The single parameter sensitivity measure was developed to measure the impact of each of the DRASTIC parameters on the DVI.

Map removal sensitivity analysis

The results of the map removal sensitivity analysis computed by removing one or more data layers at a time are presented in Table 7. The highest sensitivity index is observed upon removal of the conductivity data layer (1.42 %), followed by the topographic slope (1.21 %). The hydraulic conductivity parameter, albeit exhibiting a low theoretical weight ($C_w = 3$) and an average rating score (mean $C_r = 3.21$), has a greater variation index upon removal from the DVI map. This result is attributed to the very high coefficient of variation (CV % = 83.88) of the conductivity layer, indicative of the extent of the variability in relation to the mean value. Interestingly, in spite of the low correlation with DVI ($r = 0.02$) and the least theoretical weight ($T_w = 1$), the topographic slope has a high variation index (1.21 %) upon removal from the DVI map. This result is in all likelihood attributed to the high mean rating score (mean $T_r = 8.87$). The trend of the variation indices is in the order: $C > T > D > R > S > I > A$, which is quite different from the order of their magnitudes of the theoretical weight, i.e., $D = I > R > A = C > S > T$. As a result, the variation index is governed by the collective impact of the large data range, the mean rating score, the theoretical weight (Babiker et al. 2005; Rahman 2008; Akbari et al. 2011), and the coefficient of variation. The variation of the vulnerability index also seems to be sensitive to the removal of the data layers of depth to water, recharge, and soil media from the computation. The sensitivity index should not be confused with the variation index, which considers the magnitude of the variation created by map removal.

Table 7 Statistics of sensitivity analysis upon single and combined parameter

	Mean	Min	Max	SD
D	1.10	0.00	4.16	0.76
R	1.12	0.00	2.96	0.72
A	0.74	0.00	2.47	0.45
S	1.07	0.00	2.28	0.69
T	1.21	0.32	2.20	0.27
I	0.96	0.00	3.31	0.60
C	1.42	0.00	2.28	0.57
A	0.74	0.00	2.47	0.45
AI	1.91	0.01	5.30	0.88
ASI	1.34	0.00	4.77	0.92
DASI	3.34	0.00	8.99	2.15
DRASI	7.26	0.02	12.27	2.49
DRASTI	8.52	0.01	13.67	3.43

Furthermore, the sensitivity index of more than one parameter was considered by removing the data layers according to their ascending sensitivity indices. Logically, the mean sensitivity index should increase gradually as more than one data layer is removed successively. Contrary to this, the removal of two layers (A and I) exhibits a greater sensitivity index than the removal of three layers (A, S and I). The growing mean sensitivity index is most likely due to the collective impact of the data range, the weight, the mean rating scores, the coefficient of variation, and the correlation with DVI.

Single parameter sensitivity analysis

In this sensitivity analysis, the theoretical weights assigned to the DRASTIC parameters are compared with the effective weights, which are a function of the single parameter value with regard to the remaining six parameters,

Table 8 Single parameter sensitivity analysis

Parameter	Theoretical weight (Wt)	Wt (%)	Effective weight (%)				Revised weight
			Mean	Min	Max	SD	
D	5	21.74	18.85	4.61	39.72	6.57	4.3
R	4	17.39	20.99	6.96	33.43	4.73	4.8
A	3	13.04	18.16	5.53	29.18	3.51	4.2
S	2	8.70	7.97	0.74	19.82	4.26	1.8
T	1	4.35	7.08	0.62	12.98	1.68	1.6
I	5	21.74	19.76	12.60	34.10	3.13	4.5
C	3	13.04	7.18	0.41	25.88	5.83	1.7

considering their weights (Babiker et al. 2005). The recharge and impact of the vadose parameters are the most effective inputs of the DRASTIC model, with the highest weight of five equivalents to 21.74 %, followed by recharge (17.39 %), aquifer media, and conductivity (13.04 %) (Table 8). The present study indicates a deviation in the effective weights compared to the theoretical weights applied to the DRASTIC model. Due to the high effective weight compared to the theoretical weight, the recharge (20.8 %) and aquifer media (18.1 %) tend to be the most effective parameters, followed by topography (7 %). The rest of the parameters exhibit less effective weights than the theoretical weight. One striking fact that emerged is that the parameters with low theoretical weights exhibited large variation in the revised weights. This result indicates the small increment in the magnitude of the revised vulnerability index. Thus, the effective weights were further used to compute the revised DRASTIC vulnerability index using the following equation:

$$\text{Revised DVI} = 4.3D_{\text{r}} + 4.8R_{\text{r}} + 4.2A_{\text{r}} + 1.8S_{\text{r}} + 1.6T_{\text{r}} + 4.6I_{\text{r}} + 1.7C_{\text{r}}.$$

The revised DVI exhibit a 6 % increase in the average vulnerability score when compared with the DVI obtained using Eq. 1.

Model validation using groundwater chemistry

Groundwater chemistry of the study area was examined through 114 samples collected from less than 300 m depth. All physicochemical parameters were measured including temperature, electrical conductivity, pH, Na, Ca, Mg, K, Cl, SO_4, HCO_3, and NO_3. The result of groundwater chemistry is presented in Table 9. The groundwaters of Saq and overlying aquifers have mineralized through long resident time, rock–water interaction, and lack of periodic recharge. The geographical distribution of Cl, SO_4, and NO_3 were compared with vulnerability maps. Attempts have been made to validate the DRASTIC model using the Cl, SO_4, and NO_3^- concentration in groundwater. Chloride and sulfate in groundwater also relate to anthropogenic activities. Nitrate is considered as the most common indicator of the anthropogenic impact on groundwater (Freeze and Cherry 1979; Trojan et al. 2003; White et al. 2013), which is why the NO_3^- concentration map is preferred as a parameter to validate the DRASTIC model (Al Adamat et al. 2003; Umar et al. 2009; Saidi et al. 2011). The distribution of major elements in the groundwater system mainly depends on the soil dynamics, the recharge rate, the groundwater movement, and the on-ground pollution loading. The average concentrations of Cl, SO_4, and NO_3^- concentration measured within each vulnerability zone (Fig. 6a) is presented with different vulnerability class. The low, medium, high, and very high vulnerability zones are represented by 5, 19, 77, and 13 sampling locations. From low to medium vulnerability, there is continuous increase in the concentrations of Cl, SO_4, and NO_3. High vulnerability zone corresponds with higher NO_3 concentration following increasing trend, while Cl and SO_4 concentrations are comparatively lower than expected. The trend of low NO_3^- concentration corresponding to a very high vulnerability class (>160) can be explained by the fact that this zone does not have agricultural land use and is thus apparently free from surface pollution loading, although high Cl and SO_4 values go well with very high vulnerability class. The second validity test was performed on three subareas, chosen on account of the agriculture land-use class (Fig. 6b). The validity test was made by correlating the vulnerability indices, Cl, SO_4, and NO_3^- concentration for three subareas supporting good agriculture. The average concentration of Cl, SO_4 and NO_3^- at subareas 1, 2, and 3 were made using 48, 30, and 16 samples. The comparison of the DVI, the revised *DVI*, and Cl, SO_4, and NO_3^- concentration shows that the pollution (NO_3^-) distribution reasonably corresponds with the pollution indices, i.e., the DRASTIC and RISK maps. This result validates the use of the DRASTIC model in the present study area with the given data set.

Pollution risk map

Various human activities and land-use types have a significant impact on the groundwater vulnerability of most of

Table 9 Groundwater chemistry analyses

Formation	Conc	Depth (m)	Temp (°C)	EC (μS/cm)	TDS (mg/l)	pH	Ca (mg/l)	K (mg/l)	Mg (mg/l)	Na (mg/l)	Cl (mg/l)	SO_4 (mg/l)	HCO_3 (mg/l)	NO_3 (mg/l)
STQ	Min	15.00	22.40	306.00	202.10	6.70	22.90	0.90	1.10	5.00	12.90	21.70	65.00	0.50
	Max	290.00	37.20	7,122.00	5,073.00	8.30	353.00	55.30	175.00	1,154.00	2,060.00	1,320.00	543.00	209.30
	Ave	131.32	26.63	2,678.26	1,765.94	7.63	154.97	19.45	67.81	346.87	604.98	385.68	162.52	39.45
Saq	Min	65.00	25.40	306.00	202.10	6.70	30.80	1.40	1.10	18.90	26.30	26.90	71.00	2.10
	Max	297.00	31.60	5,443.00	4,098.00	9.60	500.20	36.10	282.90	816.20	1,373.00	1,550.00	438.00	204.60
	Ave	188.96	28.16	1,455.68	952.97	7.61	122.33	6.72	26.08	162.51	264.32	238.17	133.47	51.24
Jauf	Min	130.00	26.20	743.00	494.40	7.20	56.70	5.80	18.40	62.70	104.10	81.00	120.00	2.70
	MAX	250.00	30.10	2,448.00	1,624.00	7.80	104.80	46.60	54.60	414.30	581.40	430.00	235.00	30.70
	Ave	190.00	27.67	1,522.67	1,023.28	7.62	89.68	20.42	39.72	196.92	288.37	275.63	149.33	12.05
Jubah	Min	120.00	27.20	674.00	398.20	7.20	53.70	5.90	15.90	43.80	95.20	70.40	80.00	33.30
	Max	150.00	27.70	1,286.00	875.00	7.60	91.40	11.80	30.90	152.10	220.00	273.00	135.00	41.50
	Ave	135.00	27.45	980.00	636.60	7.40	72.55	8.85	23.40	97.95	157.60	171.70	107.50	37.40
Kahfah	Min	30.00	26.90	427.00	272.70	6.80	22.90	0.90	8.80	33.70	23.30	21.70	85.00	4.50
	Max	250.00	34.10	9,902.00	6,788.00	7.90	429.00	25.20	142.50	1,640.00	2,460.00	1,830.00	173.00	120.00
	Ave	136.88	29.49	2,801.63	1,854.19	7.55	154.25	8.33	43.96	398.31	576.83	483.10	135.25	51.24
Khuff	Min	192.00	30.70	744.00	368.60	7.10	51.10	5.60	10.10	70.40	94.90	84.30	95.00	30.10
	Max	250.00	36.80	1,797.00	1,217.00	8.30	171.00	10.10	33.20	266.20	420.00	512.50	200.00	45.50
	Ave	250.00	36.80	1,797.00	1,217.00	8.30	171.00	10.10	33.20	266.20	420.00	512.50	200.00	45.50
Quwa	Min	85.00	26.60	2,148.00	1,282.00	7.40	45.60	7.90	39.60	322.20	223.70	225.50	81.00	0.50
	Max	240.00	28.70	4,760.00	3,744.00	7.80	217.20	68.10	335.50	483.10	926.80	2,120.00	170.00	45.80
	Ave	175.67	27.83	3,457.33	2,322.67	7.57	155.07	28.70	163.47	378.83	538.17	967.83	125.67	16.47

the area (Foster 1987; Zwahlen 2004; Al-Al Hanbali and Kondoh 2008; Umar et al. 2009). According to Civita (1994), integrated vulnerability can be obtained by overlying a representation of the actual pollution sources. These sources of pollution are subdivided on the basis of their pollution potential on the intrinsic vulnerability map (Babiker et al. 2005). A land-use map with five land-use classes was obtained using the MODIS data. These land-use classes are assigned a unique rating, depending on their anticipated role as a pollution input to the groundwater environment (Table 10). The urban and agriculture land-use classes are restricted in their geographical extents, with only 0.93 and 11.63 %, respectively, of the total area assigned high ratings. The risk map is obtained by combining the land-use data layer with the modified DVI, which is computed using the revised (effective) weights:

$$\text{Risk Map Index} = \text{revised DVI} + (LU_r + LU_w),$$

where LU_r and LU_w are the land-use ratings and weight, respectively. The revised DVI is the DRASTIC vulnerability index obtained by using the revised weights.

The risk map or the integrated vulnerability map distinguishes areas carrying pollution stresses. The risk index

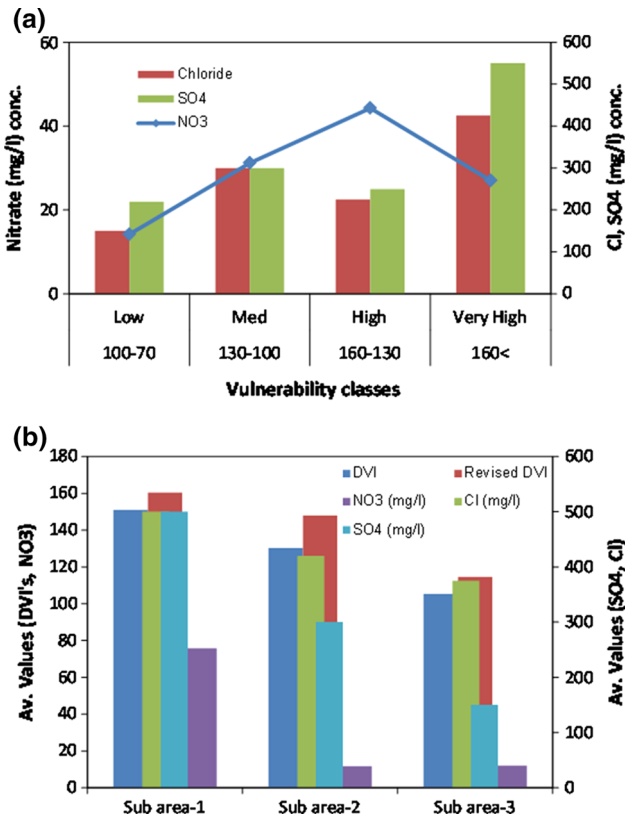

Fig. 6 Validation of DRASTIC model through comparing **a** averaged Cl, SO_4, and NO_3 concentrations in different vulnerability classes and **b** DVI, revised DVI, and averaged Cl, SO_4, and NO_3 concentrated in selected subareas

Table 10 Land-use pattern in relation to groundwater vulnerability

Land-use classes	Area (Km^2)	%	Rating
Barren rocks	55,997	13.35	1
Barren soil	98,809	23.55	2
Sand dune	211,976	50.53	3
Agriculture	48,792	11.63	8
Urban	3,910	0.93	9
Total study area	419,484	100.00	

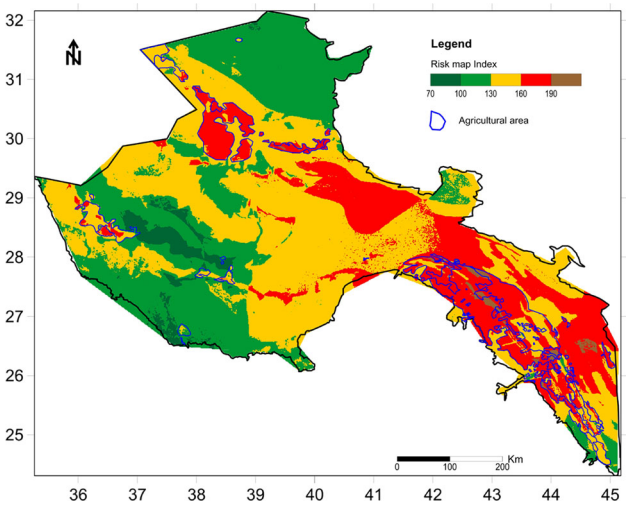

Fig. 7 Integrated vulnerability (risk map) of the study area

is classified into five classes (Fig. 7), starting from very low (70–100), low (100–130), medium (130–160), and high (160–190) to very high (>190). The boundary overlay of the agricultural areas over the risk map reveals that subareas 1 and 2 fall within the high-risk zone, while subarea 3 is situated over the medium-risk zone. The very high class extent is small and restricted to the eastern part, coinciding with few geological formations. In the southeastern part, the Saq, Minjur, and alluvial deposits lie within the high-risk zone. Some areas occupied by alluvial deposits, calcareous duricrust fall within the very high risk zone of groundwater contamination. The northwestern part of the study area, alluvial deposits, Jauf formation, and Jubbah formation lie within the high-risk zone of groundwater contamination. Tawil formation and exposed Saq at southern part lie within medium- to high-risk zone of groundwater contamination.

Conclusions and recommendations

This study assessed the groundwater vulnerability zones where contamination can occur, depending upon the combined nature of the hydrogeological environment. The hydrogeological environment of the Saq and the overlying

aquifers is conceptualized using seven data layers. Due to large extents of the study area, the data layer, except for the impact of vadose, is extremely variable. All DRASTIC data layers are independent and variable, which reduces the output errors. The recharge potential of the study area is computed using the index overlay technique, considering the details of geology, drainage, slope, and rainfall. The soil data layer was generated from the detailed soil properties, which include the use, arability, type, water retention, and conductivity. The present DRASTIC model sensitivity, defined in terms of the variation index, is attributed to one or more reasons, i.e., due to the mean rating and the coefficient of variation of the data layers. The sensitivity analysis indicated that the vulnerability index is particularly sensitive to the removal of the hydraulic conductivity and the topographic slope. The DRASTIC vulnerability map classifies the area into low, medium, high, and very high vulnerability zones. The model calibration is performed with the help of the sensitivity analysis, and the revised weights were used to obtain the integrated vulnerability map, which includes the land-use data layer. The effective weights differ from the theoretical weights, suggesting a revision of the particular parameter layers.

The validation of the model is performed using the NO_3 concentration, which is considered as a good indicator of the human interaction with the groundwater environment. A comparison of the averaged vulnerability index and the NO_3 concentration in each zone exhibits a good correlation and hence provides modal validation with the present input conditions. The integrated vulnerability map combines the risk of pollutant loading from certain sources identified on the land-use classification map. The boundary overlay of the agricultural areas over the risk map reveals that subareas 1 and 2 fall within the high-risk zone, while subarea 3 is situated over the medium-risk zone. The very high class extent is small and restricted in the eastern part, coinciding with few geological formations. The alluvial deposits, Minjur, Saq, Jauf, and Jubbah formations lie within the high-risk zone of groundwater contamination.

The vulnerability maps are useful in the implementation and prioritization of policies for aquifer protection, in particular, and water resources management, in general. The following remedial measures can be adopted to protect groundwater contamination in areas of known pollution threats:

1. Application of agricultural pesticides or chemical fertilizers should be performed in a manner that minimizes the chances for exposure to the groundwater environment.
2. A ground check should be performed to ensure safe in-house waste disposal and sewer network systems of small and large townships. Policy should be implemented to discourage the indiscriminate disposal of wastes, especially in unlined sewers and pits.
3. Areas where deep aquifers are outcropped should be given strong vigilance against pollution attenuation, irrespective of their current vulnerability class.
4. Regular monitoring of the groundwater quality should occur, especially in the areas corresponding to high to very high vulnerability classes.
5. The results of the study highlight the need to monitor the environmental impact of pesticides, chemical fertilizers, and wastewater disposal systems associated with human settlements and industries in the eastern part of the study area.

Acknowledgments This project was supported by NSTIP strategic technologies program number (12-WAT 2453-02) in the Kingdom of Saudi Arabia.

References

Al Adamat RAN, Foster IDL, Baban SNJ (2003) Groundwater vulnerability and risk mapping for the Basaltic aquifer of the Azraq basin of Jordan using GIS, Remote sensing and DRASTIC. Appl Geogr 23:303–324

Al Bassam A (2006) Evaluation of groundwater quality in Al Qassim area, Saudi Arabia, using cluster and factor analyses. Kuwait J. Sci Eng 33(2):101–121

Al Dabbagh ME (2013) Effect of tectonic prominence and growth of the Arabian shield on Paleozoic sandstone successions in Saudi Arabia. Arab J Geosci 6:835–843

Al-Dabbagh ME, Rogers JJW (1983) Depositional environments and tectonic significance of the Wajid sandstone of Saudi Arabia. J Afr Earth Sci 1:47–57

Al Hanbali A, Kondoh A (2008) Groundwater vulnerability assessment and evaluation of human activity impact (HAI) within the Dead Sea groundwater basin, Jordan. Hydrogeol J 16:499–510

Alam F, Umar R, Ahmed S, Dar FA (2012) A new model (DRASTIC-LU) for evaluating groundwater vulnerability in parts of central Ganga Plain, India. Arab J Geosci. doi: 10.1007/s12517-012-0796-y

Aller L, Bennet T, Lehr JH, Petty RJ (1987) DRASTIC: A standardized system for evaluating groundwater pollution potential using hydro geologic settings. USEPA document no. EPA/600/2-85-018

Al-Salamah IS, Ghazaw YM, Ghumman AR (2011) Groundwater modeling of Saq Aquifer Buraydah Al Qassim for better water management strategies. Environ Monit Assess 173:851–860

Al Saud M (2010) Mapping potential areas for groundwater storage in Wadi Aurnah Basin, western Arabian Peninsula, using remote sensing and geographic information system techniques. Hydrol J 18:1481–1495

Akbari GH, Shahrbabaki MR (2011) Sensitivity analysis of water at higher risk subjected to soil contaminations. Comp Meth Civil Eng 2(1):83–94

Babiker IS, Mohammed MAA, Hiyama T, Kato K (2005) A GIS-based DRATIC model for assessing aquifer vulnerability in Kakamigahara Heights, Gifu Prefecture, central Japan. Sci Total Environ 345:127–140

Bastiaansen W, Menenti R, Feddes R, Holtslag A (1998) A remote sensing surface energy balance algorithm for lands (SEBAL). J Hydrol 212:198–229

Brown GF, Schmidt DL, Huffman Jr AC (1989) Geology of the Arabian Peninsula, shield area of Western Saudi Arabia. United States Geological Survey Professional Paper 560(A):188

Chenini I, Mammou AB (2010) Groundwater recharge study in arid region: an approach using GIS techniques and numerical modeling. Comput Geosci 36:801–817

Civita M (1994) Vulnerability maps of aquifers subjected to pollution: theory and practice. Pitagora Editrice, Bologna

Doerfliger N, Zwahlen F (1997) EPIK: a new method for outling of protection areas in karstic environment. In: International symposium on karst waters and environmental impacts: pp 117–123

Edet A (2014) An aquifer vulnerability assessment of the Benin Formation aquifer, Calabar, southeastern Nigeria, using DRASTIC and GIS approach. Environ Earth Sci 71:1747–1765

El Maghraby MMS, Ahmad KO, El Nasr A, Hamouda MSA (2013) Quality assessment of groundwater at south Al Madinah Al Munawarah area, Saudi Arabia. Environ Earth Sci 70:1525–1538

Evans BM, Myers WL (1990) A GIS-based approach to evaluating regional groundwater pollution potential with DRASTIC. J Water Soil Conserv March April: 242–245

Foster SSD (1987) Fundamental concepts in aquifer vulnerability, pollution risk and protection strategy. In: van Duijvenbooden W, HG van Waegeningh (eds) Vulnerability of soil and groundwater to pollutants, Processing and Information. TNO committee on hydrological research, The Hague, 38:pp 69–86

Freeze RA, Cherry JA (1979) Groundwater: prentice hall. Englewood Cliffs, New Jersey

Gogu RC, Dassargues A (2000) Sensitivity analysis for the EPIK method of vulnerability assessment in a small karstic aquifer. South Belg Hydrogeol J 8(3):337–345

Güler C, Kurt MA, Alpaslan M, Akbulut C (2012) Assessment of the impact of anthropogenic activities on the groundwater hydrology and chemistry in Tarsus coastal plain (Mersin, SE Turkey) using fuzzy clustering, multivariate statistics and GIS techniques. J Hydrol 414:435–451

Hoetzl H (1995) Groundwater recharge in an arid karst area, Saudi Arabia, Application of Tracers in Arid zone Hydrology (Proceedings of Vienna Symposium). IAHS publ. pp 232

Huan H, Wang J, Teng Y (2012) Assessment and validation of groundwater vulnerability to nitrate based on a modified DRASTIC model: a case study in Jilin City of northeast China. Sci Total Environ 440:14–23

Hussain MH, Singhal DC, Joshi H, Kumar S (2006) Assessment of groundwater vulnerability in tropical alluvial interfluves. India Bhu Jal News 1–4:31–43

Jamrah A, Al-Futaisi A, Rajmohan N, Al-Yaroubi S (2008) Assessment of groundwater vulnerability in the coastal region of Oman using DRASTIC index method in GIS environment. Environ Monit Assess 147:125–138

Krishnamurthy J, Srinivas G (1995) Role of geological and geomorphological factors in ground water exploration: a study using IRS LISS data. Int J Remote Sens 16(14):2595–2618

Laboun AA (2013) Regional tectonic and megadepositional cycles of the Paleozoic of northwestern and central Saudi Arabia. Arab J Geosci 6:971–984

Lodwick WA, Monson W, Svoboda L (1990) Attribute error and sensitivity analysis of map operations in geographical information systems: suitability analysis. Int J Geogr Inf Syst 4(4):413–428

Memon A, Kazi A, Powell WJ, Bazuhair AS (1986) Estimation of groundwater recharge in wadi al Yammaniyah, Saudi Arabia. Environ Geol Water Sci 8(3):153–160

Mendizabal I, Stuyfzand PJ (2011) Quantifying the vulnerability of well fields towards anthropogenic pollution: the Netherlands as an example. J Hydrol 398(3):260–276

Merchant JW (1994) GIS-based groundwater Pollution hazard assessment a critical review of the DRASTIC model. Photogramm Eng Remote Sens 60(9):1117–1127

Milnes E (2011) Process-based groundwater salinisation risk assessment methodology: application to the Akrotiri aquifer (Southern Cyprus). J Hydrol 399(1):29–47

Ministry of Water and Electricity (MoWE), Saudi Arabia (2008) Investigations for updating the groundwater mathematical models of the Saq and overlying aquifers. Kingdom of Saudi Arabia: Unpublished report on file, Ministry of Water and Electricity

Napolitano P, Fabbri AG (1996) Single-parameter sensitivity analysis for aquifer vulnerability assessment using DRASTIC and SINTACS. Proceedings of the Vienna conference on HydroGIS 96: application of geographic information systems in hydrology and water resources management. IAHS 235:559–566

Navlur KCS, Engel B (1997) Predicting spatial distribution of vulnerability of Indiana State Aquifer system to nitrate leaching using GIS. http://www.ncgia.ucsb.edu/conf/SANTA_FE_CDROM/sf_papers/navulur_kumar/my_paper.html

Nazzal Y, Ahmed I, Al Arifi NSN, Ghrefat H, Zaidi FK, Waheidi El, Batayneh A, Zumlot T (2014a) A pragmatic approach to study the groundwater quality suitability for domestic and agricultural usage, saq aquifer, northwest of Saudi Arabia. Environ Monit Assess. doi:10.1007/s10661-014-3728-3

Nazzal Y, Ahmed I, Al Arifi SN, Ghrefat H, Batayneh A, Abuamarah BA, Zaidi FK (2014b) A combined hydrochemical-statistical analysis of Saq aquifer, northwestern part of the Kingdom of Saudi Arabia. Geosci J. doi:10.1007/s12303-014-0016-8

Neshat A, Pradhan B, Dadras M (2014) Groundwater vulnerability assessment using an improved DRASTIC method in GIS. Resour Conserv Recycl 86:74–86

Pathak DR, Hiratsuka A, Awata I, Chen L (2009) Groundwater vulnerability assessment in shallow aquifer of Kathmandu Valley using GIS-based DRASTIC model. Environ Geol 57:1569–1578

Powers RW, Ramirez LF, Redmond CD, Elberg EL (1966) Sedimentary Geology of Saudi Arabia. US Geological Survey Professional Paper 560-D. US Government Printing Office

Qinghai G, Yanxin W, Xubo G, Teng M (2007) A new model (DRARCH) for assessing groundwater vulnerability to arsenic contamination at basin scale: a case study in Taiyuan basin, northern China. Environ Geol 52:923–932

Rahman A (2008) A GIS based DRASTIC model for assessing groundwater vulnerability in shallow aquifer in Aligarh, India. Appl Geogr 28:32–53

Rosen L (1994) Study of the DRASTIC methodology with the emphasis on Swedish conditions. In Program and abstracts of the 37th conference of the International Association for Great Lakes Research and Estuarine Research Federation, IAGLR ,Buffalo, NY, 166

Saidi S, Bouri S, Dhia HB (2011) Sensitivity analysis in groundwater vulnerability assessment based on GIS in the Mahdia-Ksour Essaf aquifer, Tunisia: a validation study. Hydrol Sci J 56(2):288–304

Sawayan AM, Allayla R (1989) Origin of saline groundwater in Wadi Ar-Rimah, Saudi Arabia. Groundwater 27:481–490

Soller DR, Berg RC (1992) A model for the assessment of aquifer contamination potential based on regional geologic framework. Environ Geol Water Sci 19:205–213

Sorichetta A, Masetti M, Ballabio C, Sterlacchini S, Beretta GP (2011) Reliability of groundwater vulnerability maps obtained through statistical methods. J Environ Manag 92(4):1215–1224

Subyani AM (2004) Use of chloride mass-balance and environmental isotopes for evaluation of groundwater recharge in the alluvial aquifer, Wadi Tharad. West Saudi Arab J Environ Geol 46:741–749

Todd DK (1980) Groundwater hydrology, 2nd edn. Wiley, New York

Trojan MD, Maloney JS, Stockinger JM, Eid EP, Lahtinen MJ (2003) Effects of land use on groundwater quality in the Anoka Sand Plain Aquifer of Minnesota. Ground Water 41(4):482–492

Umar R, Ahmed I, Alam F (2009) Mapping groundwater vulnerable zones using modified DRASTIC approach of an alluvial aquifer in parts of Central Ganga Plain, Western Uttar Pradesh. J Geol Soc India 73:193–201

Van Stempvoort D, Evert L, Wassenaar L (1993) Aquifer vulnerability index: a GIS compactable method for groundwater vulnerability mapping. Can Water Res J 18:25–37

Vias JM, Andrco B, Perles MJ, Carrasco F, Vadillo I, Jimenez P (2006) Proposed method of groundwater vulnerability mapping in carbonate (karstic) aquifers: the COP method, Applications in two pilot sites in southern Spain. Hydrogeol J 14(6):912–925

Vrba J, Zaporotec A (eds) (1994) Guidebook on mapping groundwater vulnerability. In: IAH International Contribution for Hydrogegology, vol. 16/94. Heise, Hannover

World Atlas (1984) Ministry of Agriculture and Water in Saudi Arabia. Water Atlas of Saudi Arabia, Riyadh

White P, Ruble CL, Lane ME (2013) The effect of changes in land use on nitrate concentration in water supply wells in southern Chester County, Pennsylvania. Environ Monit Assess 185:643–651

Zwahlen F (ed) (2004) COST Action 620: vulnerability and risk mapping for the protection of carbonate (karst) aquifers, Final report. Office of the Official Publications of the European Communities, Brussels, Belgium, p 297